Electronic Supplementary Information

Nanoscaled Tin Dioxide Films Processed From Organotin-based Hybrid Materials: An Organometallic Route Toward Metal Oxide Gas Sensors

Laetitia Renard,[a] Odile Babot, [a] Hassan Saadaoui,[b] Hartmut Fuess, [c] Joachim Brötz, [c] Aleksander Gurlo,[c] Emmanuel Arveux,[c] Andreas klein,[c] and Thierry Toupance*[a]

[a] *Institut des Sciences Moléculaires, ISM UMR 5255 CNRS Groupe Matériaux, University of Bordeaux, 33405 Talence Cédex, France. Fax: + 33 5 40006994; Tel: + 33 5 40002523; E-mail: t.toupance@ism.u-bordeaux1.fr*

[b] *Centre de Recherche Paul Pascal, CRPP UPR8641 CNRS, 33600 Pessac, France. Fax : + 33 5 56845600; Tel: + 33 5 56845632.*

[c] *Fachbereich Material- und Geowissenschaften, Technische Universitaet Darmstadt, 64287 Darmstadt, Germany. Fax: + 49 6151 166346; Tel:+ 49 6151 166342.*

Characterization of the hybrid thin films

The complete hydrolysis of precursors **1** and **2** in the spin-coated hybrid thin films was checked by FTIR spectroscopy. For instance, the stretching vibration band of the Sn-C≡C bond at 2169 cm^{-1}has disappeared in the thin film prepared from **1** after drying at 120°C for one hour (Figure S1) showing that all the alkynyl groups have been removed.

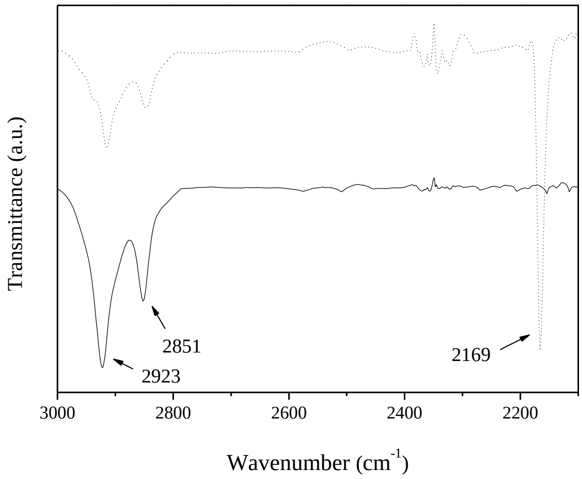

Figure S1: FTIR spectra of **1** (dotted line) and $TF_{\mathbf{1}}^{120}$ (full line).

Furthermore, the GIXRD patterns of the hybrid thin films showed diffraction features at rather low angle consistent with the formation of self-assembled tin-based hybrid thin film as described in *Chem. Commun.* **2011**, *47*, 1464.

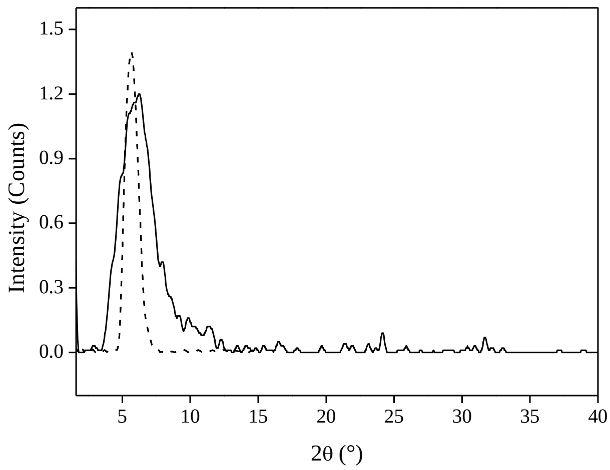

Figure S2: GIXRD patterns of $TF_{\mathbf{1}}^{120}$ (full line) and $TF_{\mathbf{2}}^{120}$ (dotted line).

Thermogravimetry coupled to mass spectrometry

The trends of molecular ion fragments as a function of the temperature detected for the hybrid material prepared from precursors **1** and **2** are given Figures S1 and S2.

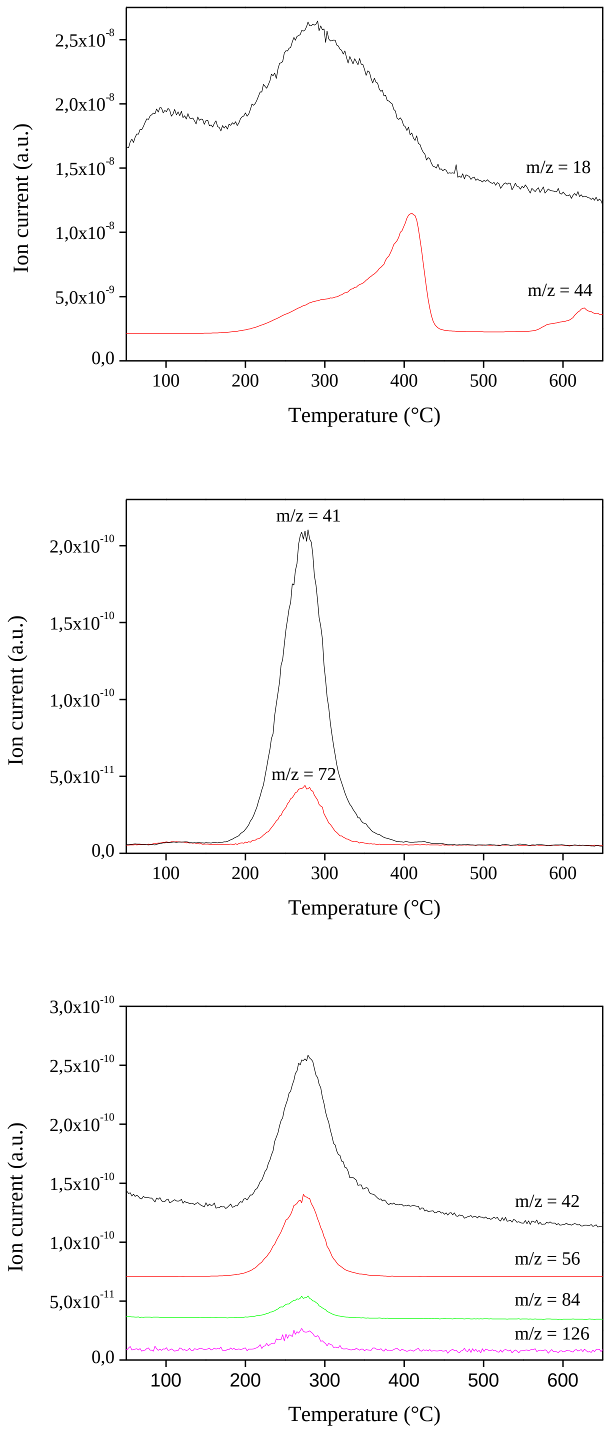

Figure S3: m/z curves as a function of temperature for the hybrid material prepared from **1** m/z = 18 (H_2O); m/z = 44 (CO_2); m/z = 41, 72 (THF); m/z = 42 ($C_3H_6^{\cdot+}$); m/z = 56 ($C_4H_8^{\cdot+}$), m/z = 84 ($C_6H_{12}^{\cdot+}$), m/z = 126 ($C_9H_{18}^{\cdot+}$).

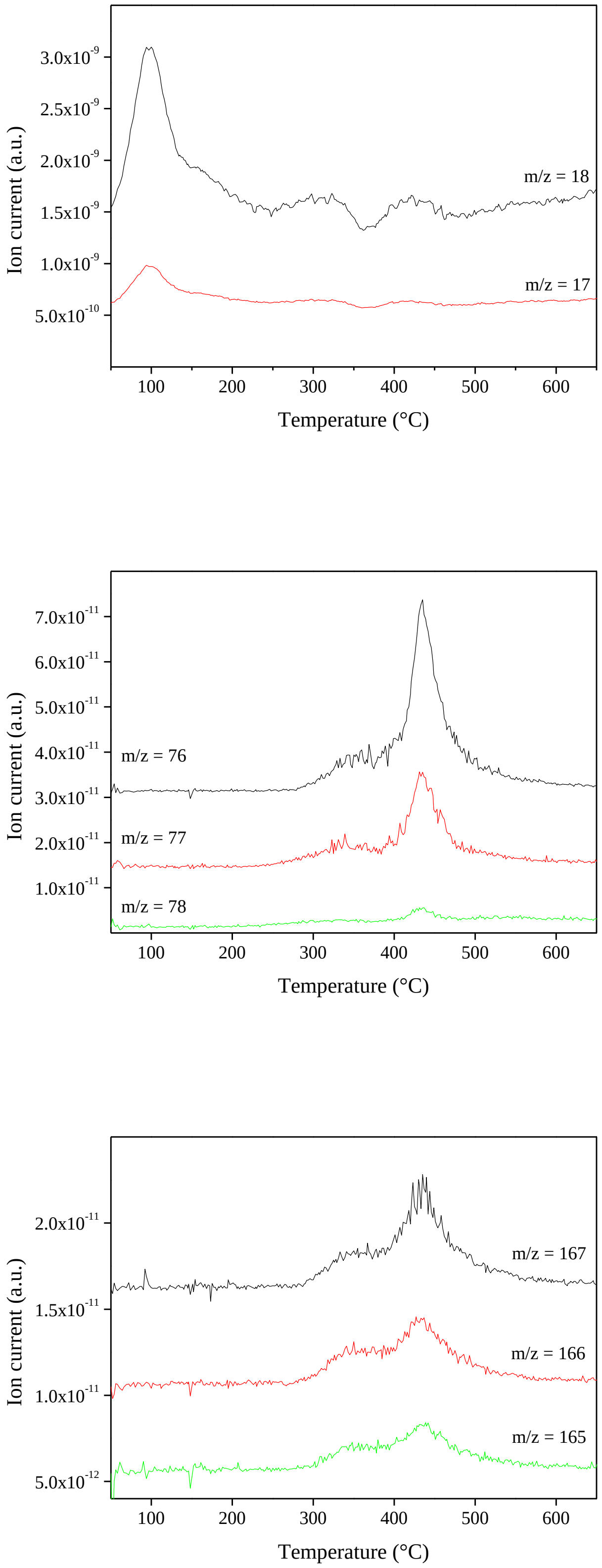

Figure S4: m/z curves as a function of temperature for the hybrid material prepared from **2** m/z = 17, 18 (H_2O); m/z = 76 ($C_6H_4^{\cdot+}$); m/z = 77 ($C_6H_5^{\cdot+}$), m/z = 78 ($C_6H_6^{\cdot+}$), m/z = 165 ($C_{13}H_9^{\cdot+}$), m/z = 166 ($C_{13}H_{10}^{\cdot+}$). m/z = 167 ($C_{13}H_{11}^{\cdot+}$).

X-ray Photoelectron Spectroscopy for thin films prepared from 2

The XPS spectra of the TF_2^{120} (**A**), TF_2^{500} (**B**) and TF_2^{600} (**C**) films are given in Figures S3 and S4.

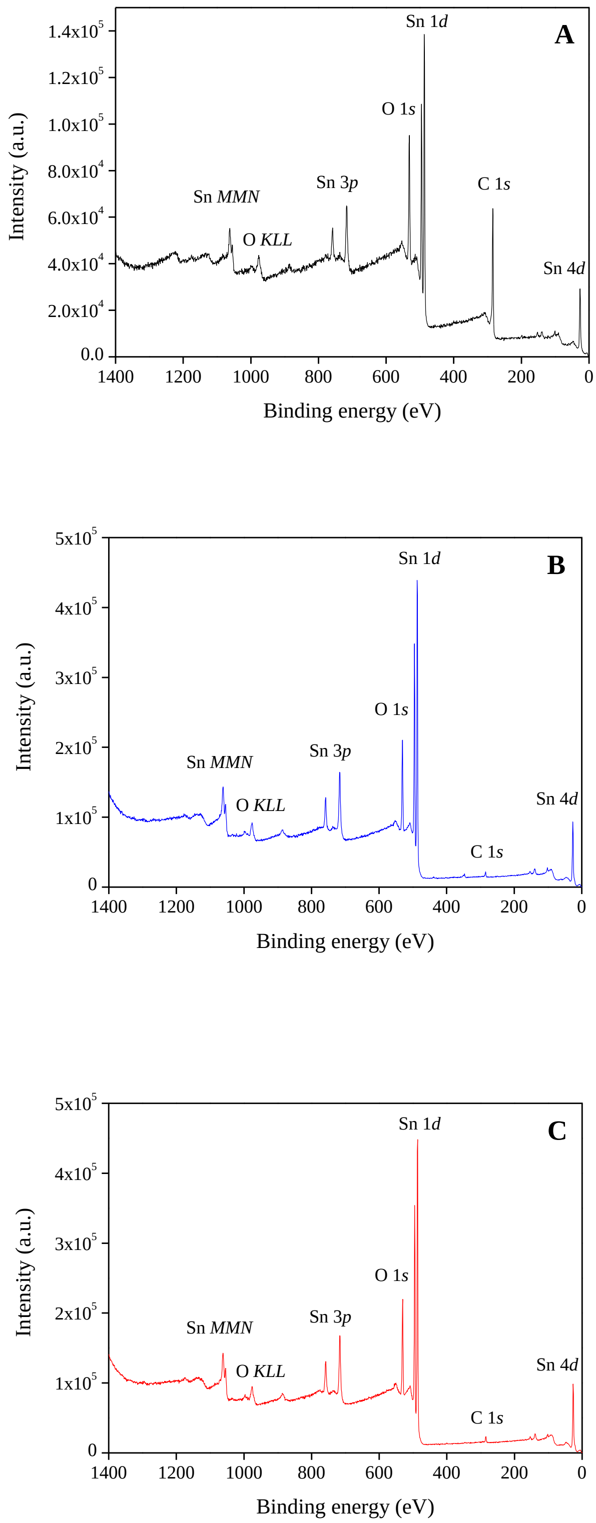

Figure S5: X-ray Photoelectron survey spectra of TF_2^{120}, TF_2^{500} and TF_2^{600}.

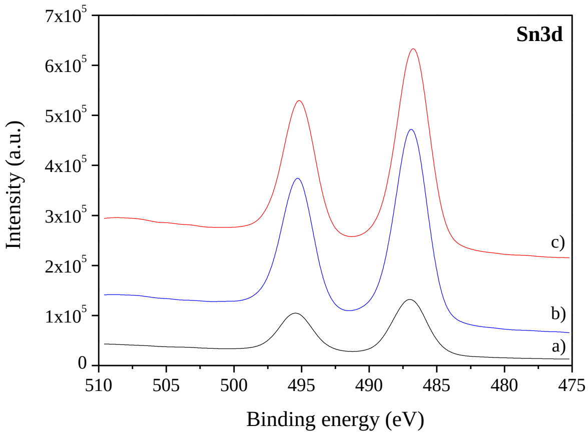

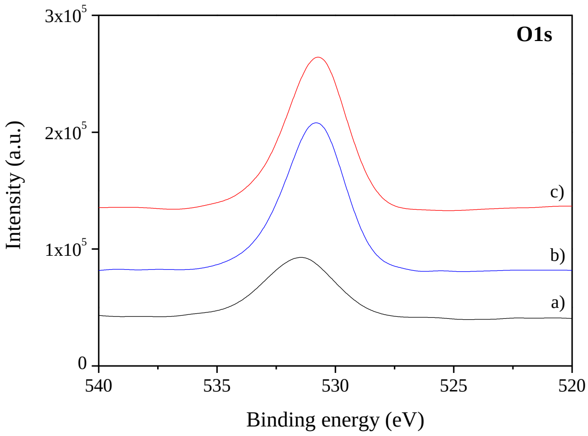

Figure S6: X-ray Photoelectron spectra of a) TF_2^{120}, (b) TF_2^{500} and (c) TF_2^{600}: Sn3d and O1s regions

Surface morphology of the TF_2^{600} film

The surface morphology of TF_2^{600} is depicted in Figure S5.

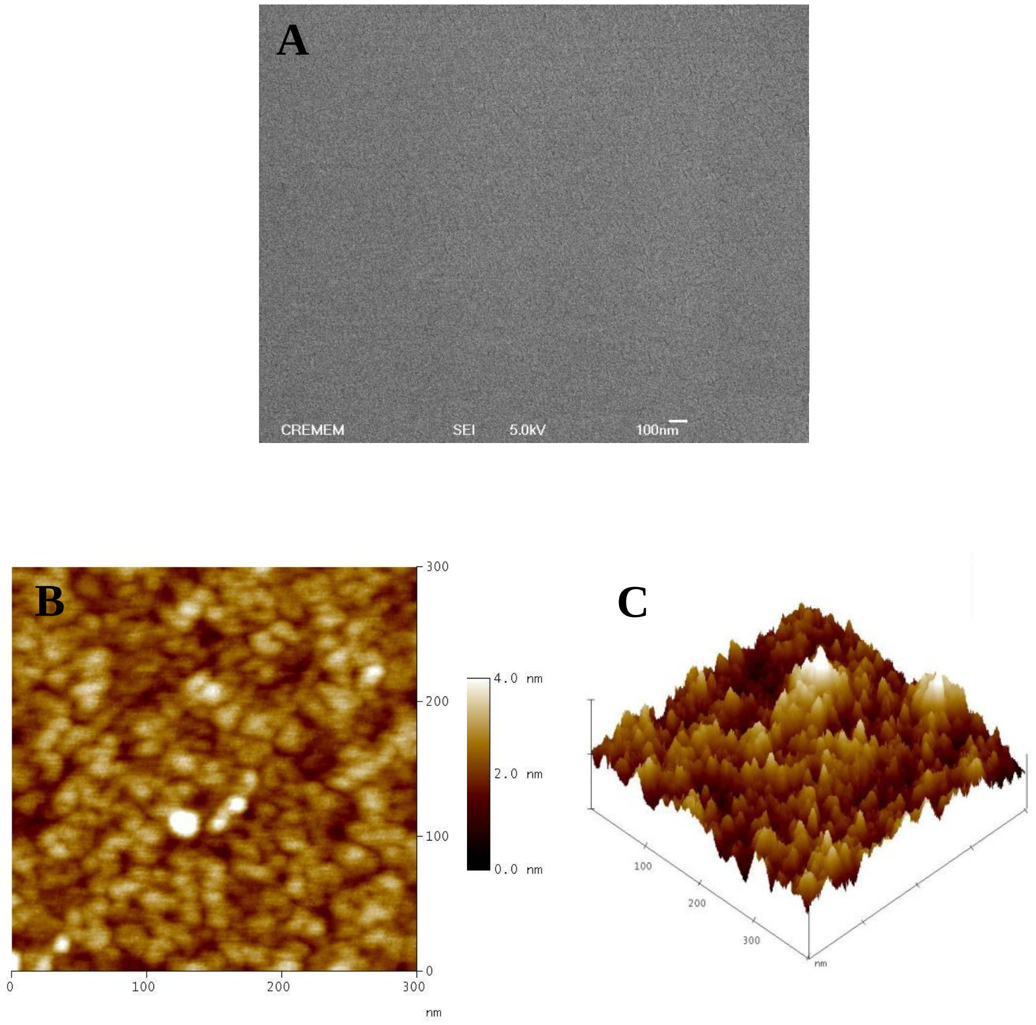

Figure S7: **A**: SEM images of TF_2^{600}; **B**, **C**: AFM topography images